Radiology

High-Grade Serous Ovarian Cancer: Associations between *BRCA* Mutation Status, CT Imaging Phenotypes, and Clinical Outcomes[1]

Stephanie Nougaret, MD, PhD[2,3]
Yulia Lakhman, MD
Mithat Gönen, PhD
Debra A. Goldman, MS
Maura Miccò, MD[4]
Melvin D'Anastasi, MD[5]
Sarah A. Johnson, MD, FRCPC[6]
Krishna Juluru, MD
Angela G. Arnold, MS
Ramon E. Sosa, BA
Robert A. Soslow, MD
Hebert Alberto Vargas, MD
Hedvig Hricak, MD, PhD
Noah D. Kauff, MD[7]
Evis Sala, MD, PhD, FRCR

Purpose: To investigate the associations between *BRCA* mutation status and computed tomography (CT) phenotypes of high-grade serous ovarian cancer (HGSOC) and to evaluate CT indicators of cytoreductive outcome and survival in patients with *BRCA*-mutant HGSOC and those with *BRCA* wild-type HGSOC.

Materials and Methods: This HIPAA-compliant, institutional review board–approved retrospective study included 108 patients (33 with *BRCA* mutant and 75 with *BRCA* wild-type HGSOC) who underwent CT before primary debulking. Two radiologists independently reviewed the CT findings for various qualitative CT features. Associations between CT features, *BRCA* mutation status, cytoreductive outcome, and progression-free survival (PFS) were evaluated by using logistic regression and Cox proportional hazards regression, respectively.

Results: Peritoneal disease (PD) pattern, presence of PD in gastrohepatic ligament, mesenteric involvement, and supradiaphragmatic lymphadenopathy at CT were associated with *BRCA* mutation status (multiple regression: $P < .001$ for each CT feature). While clinical and CT features were not associated with cytoreductive outcome for patients with *BRCA*-mutant HGSOC, presence of PD in lesser sac (odds ratio [OR] = 2.40) and left upper quadrant (OR = 1.19), mesenteric involvement (OR = 7.10), and lymphadenopathy in supradiaphragmatic (OR = 2.83) and suprarenal para-aortic (OR = 4.79) regions were associated with higher odds of incomplete cytoreduction in *BRCA* wild-type HGSOC (multiple regression: $P < .001$ each CT feature). Mesenteric involvement at CT was associated with significantly shorter PFS for both patients with *BRCA*-mutant HGSOC (multiple regression: hazard ratio [HR] = 26.7 $P < .001$) and those with *BRCA* wild-type HGSOC (univariate analysis: reader 1, HR = 2.42, $P < .001$; reader 2, HR = 2.61; $P < .001$).

Conclusion: Qualitative CT features differed between patients with *BRCA*-mutant HGSOC and patients with *BRCA* wild-type HGSOC. CT indicators of cytoreductive outcome varied according to *BRCA* mutation status. Mesenteric involvement at CT was an indicator of significantly shorter PFS for both patients with *BRCA*-mutant HGSOC and those with *BRCA* wild-type HGSOC.

Online supplemental material is available for this article.

[1] From the Department of Radiology (S.N., Y.L., M.M., M.D., S.A.J., K.J., R.E.S., H.A.V., H.H., E.S.), Department of Epidemiology and Biostatistics (M.G., D.A.G.), Clinical Genetics Service, Department of Medicine (A.G.A., N.D.K.), and Department of Pathology (R.A.S.), Memorial Sloan-Kettering Cancer Center, New York, NY. Received August 9, 2016; revision requested October 25; final revision received March 15, 2017; accepted March 18; final version accepted March 23. **Address correspondence to** S.N. (e-mail: *stephanienougaret@free.fr*).

Y.L., M.G., D.A.G., K.J., A.G.A., R.E.S., R.A.S., H.A.V., H.H., and E.S. supported by National Institute of Health and National Cancer Institute (grant P30 CA 008748). S.N. supported by INCa-SIRIC.

Current addresses:
[2] Department of Radiology, Institut Régional du Cancer de Montpellier, Montpellier, France.
[3] IRCM, Institut de Recherche en Cancérologie de Montpellier, Montpellier, France. INSERM, U1194, Montpellier, France.
[4] Department of Bioimaging and Radiological Science, Catholic University "A. Gemelli" Hospital, Rome, Italy.
[5] Department of Clinical Radiology, Ludwig-Maximilians-University Hospitals Munich-Campus Grosshadern, Munich, Germany.
[6] Department of Medical Imaging, Princess Margaret Cancer Cente, University of Toronto, Toronto, Ont, Canada.
[7] Clinical Cancer Genetics Program, Duke Cancer Institute, Duke University Health System, Durham, NC.

S.N. and Y.L. contributed equally to this work.

In 2017, it is estimated that 22440 women in the United States will be diagnosed with epithelial ovarian cancer, and 14240 will succumb to the disease (1). Primary ovarian, fallopian tube, and peritoneal high-grade serous ovarian cancer (HGSOC) is the most prevalent and lethal histologic subtype of epithelial ovarian cancer, partly because it is frequently diagnosed at advanced stages (2). Nearly all HGSOC harbor a mutation in the p53 gene and a large number of gene copy alterations (3–5). Other repeated mutations most commonly include a mutation in either the *BRCA1* or *BRCA2* gene. *BRCA* germline mutations are reported in 15%–17% of HGSOC, while somatic mutations are observed in 6% of HGSOC (6,7).

Several studies have suggested that patients with *BRCA*-mutant HGSOC have improved survival compared with those with *BRCA* wild-type HGSOC (8–14). More favorable prognosis of *BRCA*-mutant HGSOC is attributed to greater platinum sensitivity in primary and recurrent settings, as well as to unique tumor biology that confers survival advantage independent of chemotherapy sensitivity (14,15). Given the substantial prognostic and therapeutic implications of *BRCA* mutation status, some researchers advocate for genetic testing in all women with a new diagnosis of HGSOC (16,17).

Recent data from histopathology literature suggest that in patients with HGSOC the morphology of both primary ovarian tumors and peritoneal implants is influenced by the presence of *BRCA* gene mutation (18,19). For example, peritoneal deposits with "pushing" or rounded contours predominate in *BRCA*-mutant HGSOC, while infiltrative implants are more frequently observed with in *BRCA* wild-type HGSOC (18). Some have raised the possibility that these morphologic differences in histopathology may influence the results of primary cytoreduction in patients with *BRCA*-mutant HGSOC.

Patients with a new diagnosis of epithelial ovarian cancer are routinely imaged with computed tomography (CT) as a part of the initial work-up. While it is clear that *BRCA* gene mutation produces characteristic morphologic differences at histopathologic examination, it is unknown if the presence of *BRCA* gene mutation translates into distinct imaging manifestations and if these can be reliably recognized at CT. Furthermore, although several studies have shown that CT features may serve as useful predictors of cytoreductive outcome in HGSOC, it is uncertain if these CT indicators vary depending on *BRCA* mutation status (20–23). Thus, the aims of our study were to investigate the associations between *BRCA* mutation status and CT phenotypes of HGSOC and to evaluate CT indicators of cytoreductive outcome and survival in patients with *BRCA*-mutant HGSOC and patients with *BRCA* wild-type HGSOC.

Advances in Knowledge

- Pattern of peritoneal disease (PD), presence of PD in gastrohepatic ligament, mesenteric involvement (MI), and supradiaphragmatic lymphadenopathy at CT were significantly associated with *BRCA* mutation status at univariate analysis and multiple regression.
- At multiple regression, nodular PD pattern (odds ratio [OR] = 7.16) and presence of PD in gastrohepatic ligament (OR = 9.16) at CT were associated with significantly higher odds of *BRCA*-mutant high-grade serous ovarian cancer (HGSOC), whereas presence of MI (OR = 0.07) and supradiaphragmatic lymphadenopathy (OR = 0.28) were associated with significantly lower odds of *BRCA*-mutant HGSOC.
- While none of the clinical and CT features were associated with cytoreductive outcome (complete vs incomplete cytoreduction) for patients with *BRCA*-mutant HGSOC, presence of PD in lesser sac (OR = 2.40) and left upper quadrant (OR = 1.19), MI (OR = 7.10), and lymphadenopathy in supradiaphragmatic (OR = 2.83) and suprarenal para-aortic (OR = 4.79) regions were associated with significantly higher odds of incomplete gross resection in *BRCA* wild-type HGSOC at multiple regression.
- MI at CT was associated with significantly shorter progression-free-survival for both patients with *BRCA*-mutant HGSOC (hazard ratio [HR] = 26.7) and those with *BRCA* wild-type HGSOC (HR = 2.42 [reader 1]; HR = 2.61 [reader 2]).

Implication for Patient Care

- CT features were associated with cytoreductive outcome (complete vs incomplete cytoreduction) only in patients with *BRCA* wild-type HGSOC, not in patients with *BRCA*-mutant HGSOC; this information may be of value for pretreatment patient counseling and initial decision making regarding maximal upfront cytoreductive effort versus neoadjuvant chemotherapy.

Materials and Methods

The institutional review board approved this retrospective Health Insurance

https://doi.org/10.1148/radiol.2017161697

Content codes: GU OB

Radiology 2017; 285:472–481

Abbreviations:
CI = confidence interval
HGSOC = high-grade serous ovarian cancer
PD = peritoneal disease
PFS = progression-free survival

Author contributions:
Guarantors of integrity of entire study, S.N., Y.L., E.S.; study concepts/study design or data acquisition or data analysis/interpretation, all authors; manuscript drafting or manuscript revision for important intellectual content, all authors; approval of final version of submitted manuscript, all authors; agrees to ensure any questions related to the work are appropriately resolved, all authors; literature research, S.N., Y.L., M.M., R.A.S., H.A.V., E.S.; clinical studies, S.N., Y.L., S.A.J., A.G.A., R.E.S., H.H., E.S.; experimental studies, S.N., M.M., K.J.; statistical analysis, Y.L., M.G., D.A.G.; and manuscript editing, S.N., Y.L., M.G., M.D., R.A.S., H.A.V., H.H., E.S.

Conflicts of interest are listed at the end of this article.

Table 1

Patients and Clinical Characteristics

Characteristic	All (n = 108)	*BRCA* Mutant (n = 33)	*BRCA* Wild Type (n = 75)	*P* Value
Age at diagnosis (y)*	58 (30–82)	55 (30–78)	59 (38–82)	.032
FIGO stage				.885
III	77 (71)	22 (67)	55 (73)	
IV	31 (29)	11 (33)	20 (27)	
CA-125 level (U/mL)*	427 (11–14200)	677 (25–12400)	401 (11–14200)	.667
Outcome of primary cytoreductive surgery				.810
Complete cytoreduction	62 (57)	17 (51.5)	45 (60)	
Incomplete cytoreduction	46 (43)	16 (48.5)	30 (40)	
≤1 cm residual disease (optimal)	36 (78)	12 (75)	24 (80)	
>1 cm residual disease (suboptimal)	10 (22)	4 (25)	6 (20)	
Relapse or progression				.15
Yes	91 (84)	25 (76)	66 (88)	
No	17 (16)	8 (24)	9 (12)	
Median follow-up (mo)*	51.5 (4–107)	51.5 (18–78)	52.0 (4–107)	.58
Median time to progression or death (mo)†	20.3 (16.9, 25.5)	21.1 (16.2, 25.8)	20.1 (16.3, 34.1)	.23

Note.—FIGO = International Federation of Gynecology and Obstetrics.

* Data in parentheses are the range.

† Data in parentheses are the 95% CIs.

Portability and Accountability Act-compliant study and waived the requirement for informed consent.

Eligibility Criteria

The inclusion criteria for our study were as follows: *(a)* pathologically confirmed stage III or IV HGSOC, *(b)* primary debulking surgery performed at our institution between November 1, 2005, and February 29, 2012, *(c)* genetic counseling and *BRCA* mutation testing, and *(d)* preoperative contrast material–enhanced CT of abdomen and pelvis. Patients who underwent neoadjuvant chemotherapy followed by interval debulking surgery were excluded because this group potentially differed from patients who underwent primary debulking surgery in terms of cytoreductive outcome and progression-free survival (PFS) in ways other than *BRCA* mutation status. Furthermore, neoadjuvant chemotherapy alters CT imaging findings. One hundred eight patients satisfied the eligibility criteria (Table 1, Fig 1).

The mean number of days between CT and surgery was 19 days (range, 1–135 days). One hundred seven of 108 patients (99%) underwent preoperative CT within 60 days of surgery. Primary debulking was performed according to our institutional surgical template and, at a minimum, included total abdominal hysterectomy, bilateral salpingo-oophorectomy, omentectomy, and pelvic/para-aortic lymphadenectomy. Additional resections were performed at the surgeons' discretion.

Some patients in our cohort were also included in several previously published studies, none of which assessed CT imaging (8,15,18,19).

Histopathologic Diagnoses

Fellowship-trained oncologic pathologists reviewed all final surgical specimens. The Gilks et al (24) modification to the World Health Organization criteria was used to diagnose HGSOC.

BRCA Testing

From 2005 to 2008, patients were referred for genetic counseling and *BRCA* testing based on at least one of the following indications: *(a)* family history of breast cancer before the age of 50 or history of ovarian cancer at any age in a first- or second-degree relative, *(b)* Eastern European (Ashkenazi) Jewish heritage, *(c)* patient request, or *(d)* physician's request (8). From July 2008 to 2012, genetic counseling and *BRCA* testing was offered to all patients with HGSOC regardless of family history (8). Testing was performed as previously described (8).

CT Technique

CT scans were obtained with multidetector CT scanners with four to 64 detector rows. Images were acquired during breath hold by utilizing the following acquisition parameters: 120 kVp; automatic milliampere setting (depending on patient size), with a range of 240–400 mA; mean section thickness of 4.7 mm (range, 1.25–7.5 mm); and pitch less than 1. All patients who were scanned at our institution received 150 mL of intravenous contrast material (iohexol 300, Omnipaque 300; Amersham Health, GE Medical Systems, Milwaukee, Wis) at a rate of 2.5 mL/sec by using a power injector. The time delay from contrast agent injection to image acquisition was approximately 70 seconds. CT examinations that were performed at outside institutions (n = 65) either met or exceeded the above technical standards. Images from all studies were transferred to a picture archiving

Figure 1

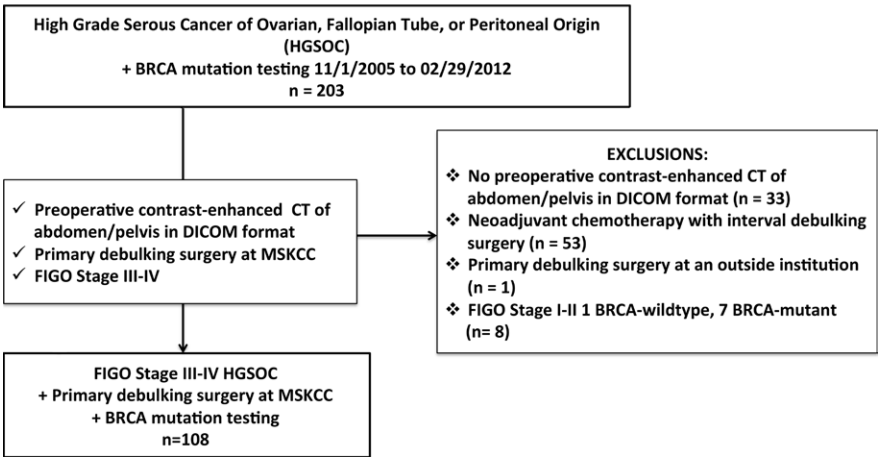

Figure 1: Flowchart shows the details of patient selection process. *DICOM* = Digital Imaging and Communications in Medicine, *FIGO* = International Federation of Gynecology and Obstetrics, *MSKCC* = Memorial Sloan Kettering Cancer Center.

and communication system (PACS) (Centricity; GE Healthcare) and were interpreted at PACS workstations.

Qualitative CT Analysis

All preoperative CT scans were independently and retrospectively interpreted by each of the two readers. Both readers were fellowship-trained radiologists with 8 (Y.L.) and 5 (S.N.) years of experience in oncologic imaging.

Assessment of primary ovarian masses.—Each reader recorded the presence of ovarian mass, its margins (smooth or irregular), internal architecture (cystic/predominantly cystic or solid/predominantly solid), and the presence of calcifications.

Assessment of extraovarian tumor spread.—Each reader noted the amount of ascites (none/small or moderate/large volume), presence of peritoneal implants, mesenteric involvement, and lymphadenopathy. Mesenteric involvement was diagnosed if either mesenteric infiltration or mesenteric nodules or both were seen (Fig 2). Mesenteric infiltration was defined as the infiltration of mesenteric fat or tethering of bowel loops along the mesentery as described previously by Vargas et al (25). When peritoneal implants were present, the predominant morphologic pattern of peritoneal disease (PD) was recorded as either nodular or infiltrative: nodular was defined as the presence of implants with predominantly well-defined or rounded or "pushing" borders, and infiltrative was defined as the presence of implants with mostly poorly defined or infiltrative borders (Fig 3).

To examine the relationship between the disease burden and cytoreductive outcome (complete or incomplete gross resection), locations of peritoneal implants were recorded. The following PD locations were evaluated: *(a)* gallbladder fossa and/or left intersegmental fissure, *(b)* gastrohepatic ligament, *(c)* lesser sac, and *(d)* left upper quadrant including gastrocolic ligament, splenic hilum, and splenic capsule. These locations were selected on the basis of their significant association with cytoreductive outcome in the study by Suidan et al (20).

The readers also assessed each CT for the presence of lymphadenopathy. The following short-axis dimensions were used to define lymphadenopathy: *(a)* supradiaphragmatic lymph nodes greater than 0.5 cm, *(b)* portocaval lymph nodes greater than 1.5 cm, and *(c)* porta hepatis (periportal) and suprarenal para-aortic lymph nodes greater than 1.0 cm. Lymph node was also considered abnormal regardless of size if it had spiculated borders or heterogeneous attenuation (other than fatty hila regions) or if nodal clustering was present.

Data Collection

Demographic, clinical, surgical, and pathologic data were collected for all patients. Recurrence or progression date was determined according to follow-up CT findings and/or CA-125 level. When diagnosed at follow-up CT, it was defined as the first appearance of one or more new tumor or enlargement of existing lesions after completion of adjuvant chemotherapy according to RECIST (Response to Treatment in Solid Tumors) (26). When determined by CA-125 level, progression date was defined as the first date when CA-125 level reached twice or more its nadir value or twice the upper limit of normal (27).

The assessment of cytoreductive outcome was performed intraoperatively by the surgeon at the conclusion of the primary cytoreductive procedure according to the standard clinical practice. Complete cytoreduction (complete gross resection) was defined as no visible residual disease at the completion of cytoreductive surgery. Conversely, incomplete cytoreduction (incomplete gross resection) was defined as any visible residual disease at the completion of cytoreductive surgery.

Statistical Analysis

Associations between clinical and pathologic characteristics versus *BRCA* mutation status were evaluated by using Fisher exact test. Interobserver agreement was analyzed with the Cohen κ statistic. The κ statistic was interpreted as follows: less than 0, no agreement; 0–0.20, slight agreement; 0.21–0.40, fair agreement; 0.41–0.60, moderate agreement; 0.61–0.80, substantial agreement; and 0.81–1.0, almost perfect agreement. We also estimated 95% confidence intervals (CIs) and reported percentage agreement between the readers.

Since only a few patients lacked peritoneal dissemination (four of 108 for both readers) or had distant

Figure 2

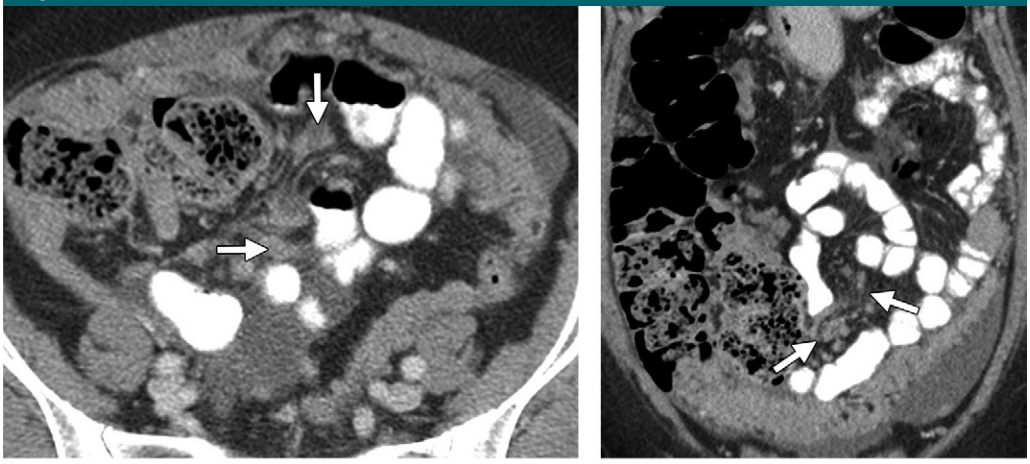

a. b.

Figure 2: Mesenteric involvement in a 63-year-old woman with *BRCA*-mutant HGSOC. **(a)** Axial and **(b)** coronal CT images demonstrate mesenteric infiltration and nodules consistent with mesenteric involvement (arrows).

Figure 3

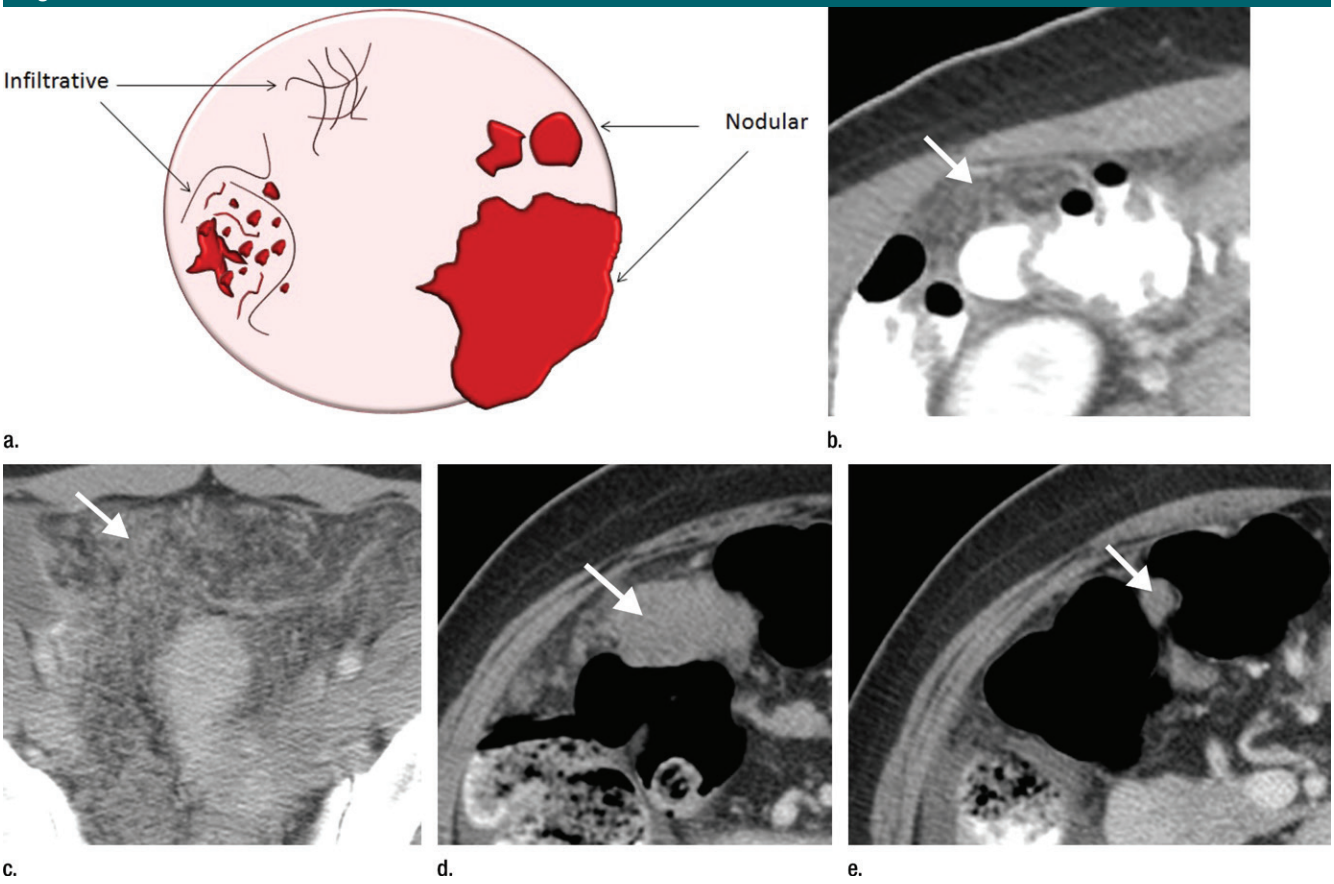

a. b.

c. d. e.

Figure 3: **(a)** Illustration of infiltrative and nodular PD patterns at CT. Axial CT images obtained in **(b)** a 55-year-old woman and **(c)** a 69-year-old woman with *BRCA* wild-type HGSOC demonstrate infiltrative PD pattern (arrow). Axial CT images in **(d)** a 68-year-old woman and **(e)** a 78-year-old woman with *BRCA*-mutant HGSOC show nodular PD pattern (arrow).

metastases (three of 108 for both readers) at CT, these CT features could not be included as covariates on univariate and multiple regression analyses.

Logistic regression was used to evaluate the relationships between CT features and *BRCA* mutation status. This analysis was performed in two steps. In the first step, we analyzed the data from each reader separately and evaluated the association between each CT feature and *BRCA* mutation status (univariate analysis). In the second step, we used only the CT features that were significantly associated with *BRCA* mutation status for both readers in the first step and built a multiple logistic regression model (multiple regression) where we used generalized estimating equations to fit the model.

Univariate Cox proportional hazards regression was used to examine the relationships between CT features and PFS separately according to *BRCA* mutation status. Patients who had a recurrence or death from any cause without documented recurrence were considered events in the PFS analysis, and their time to progression was calculated as the interval between surgery and progression or death. Patients who were alive and recurrence free at the time of analysis were considered censored, and their time to progression was calculated as the interval between surgery and their last follow-up. The median follow-up time was 51.5 months (range, 4–107 months) and the median time to progression or death was 20.3 months (95% CI: 16.9 months, 25.5 months).

All analyses were performed by using SAS 9.4 (SAS Institute, Cary, NC) and R 3.1.2 (The R Foundation) software.

Table 2

Interobserver Agreement Regarding Qualitative CT Features

CT Feature	Agreement (%)	κ Value	95% CI
Primary ovarian mass			
Mass presence	100.0	1.00	1.00, 1.00
Margins	85.1	0.65	0.48, 0.81
Architecture	91.5	0.83	0.71, 0.94
Calcifications	95.7	0.64	0.32, 0.97
PD			
Amount of ascites	96.3	0.92	0.84, 1.00
PD presence	100.0	1.00	1.00, 1.00
Gallbladder fossa/left intersegmental fissure	97.2	0.91	0.82, 1.00
Gastrohepatic ligament	91.7	0.77	0.63, 0.91
Lesser sac	97.2	0.93	0.84, 1.00
Left upper quadrant	96.3	0.92	0.85, 1.00
PD pattern (nodular or infiltrative)	90.4	0.80	0.68, 0.91
Mesenteric involvement	93.5	0.87	0.77, 0.96
Lymphadenopathy			
Periportal	97.2	0.90	0.78, 1.00
Supradiaphragmatic	97.2	0.94	0.88, 1.00
Suprarenal para-aortic	96.3	0.88	0.77, 0.99
Distant metastases	100.0	1.00	1.00, 1.00

Results

Patient Characteristics

Patient and tumor characteristics are summarized in Table 1. Our study included 108 women (median age, 58 years; range, 30–82 years), 33 (31%) of whom had *BRCA*-mutant HGSOC and 75 (69%) had *BRCA* wild-type HGSOC. Among the 33 women with *BRCA*-mutant HGSOC, 21 (63.6%) had *BRCA1* mutation and 12 (36.4%) had *BRCA2* mutation.

Interobserver Agreement

As detailed in Table 2, interobserver agreement with regard to CT features ranged from substantial to almost perfect (k = 0.64–1.00) and included substantial agreement for ovarian mass margins (k = 0.65; 95% CI: 0.48, 0.81), ovarian mass calcifications (k = 0.64; 95% CI: 0.32, 0.97), and PD pattern (k = 0.80; 95% CI: 0.68, 0.91) and almost perfect agreement for multiple other CT features including mesenteric involvement (k = 0.87; 95% CI: 0.77, 0.96).

Associations between CT Features and *BRCA* Mutation Status

At univariate analysis, no significant associations were found between *BRCA* mutation status and CT features of ovarian masses, amount of ascites, most locations of PD, or most locations of lymphadenopathy (P = .173–.948) (Table 3).

In contrast, PD pattern (reader 1: P = .001; reader 2: $P < .001$), presence of PD in gastrohepatic ligament (reader 1: P = .022; reader 2: P = .025), mesenteric involvement ($P < .001$ both readers), and supradiaphragmatic lymphadenopathy (reader 1: P = .009; reader 2: P = .004) were significantly associated with *BRCA* mutation status for both readers (Table 3).

At multiple regression, PD pattern, presence of PD in gastrohepatic ligament, mesenteric involvement, and supradiaphragmatic lymphadenopathy remained significantly associated with *BRCA* mutation status ($P < .001$ each CT feature) (Table 4). In particular, nodular PD pattern (odds ratio [OR] = 7.16) and presence of PD in gastohepatic ligament (OR = 9.16) were associated with significantly higher odds of *BRCA*-mutant HGSOC, whereas mesenteric involvement (OR = 0.07) and supradiaphragmatic lymphadenopathy (OR = 0.28) were associated with significantly lower odds of *BRCA*-mutant HGSOC (Table 4).

Associations between CT Features and Cytoreductive Outcome (Complete versus Incomplete Cytoreduction)

For patients with *BRCA*-mutant HGSOC at univariate analysis, we found no significant associations between

Table 3

Univariate Analysis of the Associations between CT Features and *BRCA* Mutation Status

	Reader 1				Reader 2			
CT Feature*	*BRCA* Mutant	*BRCA* Wild Type	Odds Ratio†	*P* Value	*BRCA* Mutant	*BRCA* Wild Type	Odds Ratio†	*P* Value
Ovary								
Ovarian mass			2.95 (0.62, 14.01)	.173			2.95 (0.62, 14.01)	.173
Present	31	63			31	63		
Absent (reference)	2	12			2	12		
Margins			0.68 (0.28, 1.68)	.408			0.66 (0.25, 1.70)	.385
Irregular	19	44			21	48		
Smooth (reference)	12	19			10	15		
Architecture			0.85 (0.36, 2.02)	.718			0.61 (0.25, 1.46)	.266
Cystic/predominantly cystic	16	35			17	42		
Solid/predominantly solid (reference)	15	28			14	21		
Calcifications			1.58 (0.33, 7.54)	.566			0.49 (0.05, 4.59)	.533
Present	3	4			1	4		
Absent (reference)	28	59			30	59		
Peritoneum								
Moderate to large ascites			1.57 (0.66, 3.69)	.305			1.47 (0.64, 3.42)	.366
Present	13	22			14	25		
Absent (reference)	20	53			19	50		
Gallbladder fossa/left intersegmental fissure			1.17 (0.42, 3.24)	.758			0.82 (0.29, 2.33)	.708
Present	7	14			6	16		
Absent (reference)	26	61			27	59		
Gastrohepatic ligament			3.00 (1.17, 7.68)	.022			2.83 (1.14, 7.02)	.025
Present	12	12			13	14		
Absent (reference)	21	63			20	61		
Lesser sac			1.74 (0.68, 4.42)	.245			1.71 (0.69, 4.21)	.247
Present	10	15			11	17		
Absent (reference)	23	60			22	58		
Left upper quadrant			1.11 (0.48, 2.54)	.813			0.96 (0.41, 2.24)	.923
Present	14	30			12	28		
Absent (reference)	19	45			21	47		
PD pattern			4.43 (1.79, 10.96)	.001			5.03 (2.03, 12.49)	<.001
Nodular	20	23			18	17		
Infiltrative (reference)	10	51			12	57		
Mesentery								
Mesenteric involvement			0.13 (0.04, 0.40)	<.001			0.10 (0.03, 0.30)	<.001
Present	4	39			4	44		
Absent (reference)	29	36			29	31		
Lymphadenopathy								
Periportal			1.04 (0.33, 3.27)	.948			0.78 (0.26, 2.37)	.659
Present	5	11			5	14		
Absent (reference)	28	64			28	61		
Supradiaphragmatic			0.27 (0.10, 0.72)	.009			0.23 (0.08, 0.62)	.004
Present	6	34			6	37		
Absent (reference)	27	41			27	38		
Suprarenal para-aortic			1.41 (0.50, 3.99)	.514			1.63 (0.62, 4.27)	.317
Present	7	12			9	14		
Absent (reference)	26	63			24	61		

* PD presence/absence and distant metastases were not included in logistic regression analyses due to small numbers of patients with absent PD or present distant metastases (as detailed in Statistical Analysis).

† Data in parentheses are the 95% CIs.

Table 4

Multiple Regression of the Associations between CT Features and *BRCA* Mutation Status

CT Feature	Odds Ratio*	*P* Value
Mesenteric Involvement	0.07 (0.06, 0.09)	<.001
PD in gastrohepatic ligament	9.16 (5.43, 15.43)	<.001
PD pattern	7.16 (5.81, 8.84)	<.001
Supradiaphragmatic lymphadenopathy	0.28 (0.20, 0.41)	<.001

* Data in parentheses are the 95% CIs.

clinical characteristics (patient age and CA-125 level at diagnosis), CT features, and cytoreductive outcome for both readers (P = .057 to >.99) (Table E1 [online]). Cytoreductive outcome was significantly associated with PD pattern for only reader 2 (P = .031) and PD in gastrohepatic ligament for only reader 1 (P = .027), but not for both readers.

For patients with *BRCA* wild-type HGSOC at univariate analysis, clinical characteristics (patient age and CA-125 level at diagnosis) were not associated with cytoreductive outcome ($P \geq .92$). In contrast, presence of moderate or large amount of ascites (reader 1: P = .033; reader 2: P = .048), PD in gallbladder fossa and/or left intersegmental fissure (reader 1: P = .012; reader 2: P = .003), lesser sac ($P < .001$ both readers), left upper quadrant ($P \leq .001$ both readers), mesenteric involvement ($P < .001$ both readers), and lymphadenopathy in supradiaphragmatic ($P \leq .001$) and suprarenal para-aortic regions (reader 1: P = .013; reader 2: P = .003) were associated with significantly higher odds of incomplete cytoreduction for both readers (Table E2 [online]).

At multiple regression, for patients with *BRCA* wild-type HGSOC, presence of PD in left upper quadrant ($P < .001$) and lesser sac ($P < .001$), mesenteric involvement ($P < .001$), and lymphadenopathy in supradiaphragmatic ($P < .001$) and suprarenal para-aortic regions ($P < .001$) remained associated with significantly higher odds of incomplete cytoreduction (Table E3 [online]).

Progression-Free Survival

For patients with *BRCA*-mutant HGSOC at univariate analysis, elevation of CA-125 (hazard ratio, 1.0003; P = .021), presence of mesentery involvement (hazard ratio, 24.46; $P < .001$ for both readers), and lymphadenopathy in periportal (hazard ratio, 4.07; P = .007 both readers) and supradiaphragmatic regions (hazard ratio, 3.14; P = .028 both readers) were associated with significantly shorter PFS for both readers (Table E4 [online]). At multiple regression, only the presence of mesentery involvement (hazard ratio, 26.7; $P <$ .001) remained associated with significantly shorter PFS.

For patients with *BRCA* wild-type HGSOC at univariate analysis, only the presence of mesenteric involvement (reader 1: hazard ratio = 2.42, $P <$ .001; reader 2: hazard ratio = 2.61, $P <$ .001) was associated with significantly shorter PFS (Table E5 [online]).

Discussion

In this study we found CT features of HGSOC to differ based on the *BRCA* mutation status. We also demonstrated that the associations between CT features, cytoreductive outcome, and PFS in HGSOC patients varied according to *BRCA* mutation status.

First, we found nodular PD pattern and presence of PD in gastrohepatic ligament to be associated with significantly higher odds of *BRCA*-mutant HGSOC at multiple regression. In contrast, infiltrative PD pattern, presence of mesenteric involvement, and supradiaphragmatic lymphadenopathy were associated with significantly lower odds of *BRCA*-mutant HGSOC at multiple regression.

The breast imaging literature supports our findings regarding the associations between morphology of peritoneal implants and *BRCA* mutation status (28,29). Primary breast tumors of *BRCA* mutation carriers often demonstrate "prominent pushing margins" thought to be related to the continuous front of tumor cells without interspersed connective tissues (29). At mammography and breast magnetic resonance (MR) imaging, these histopathologic findings translate into characteristic imaging manifestations: breast tumors in *BRCA* mutation carriers show predominantly rounded or well-defined margins, whereas breast masses that arise sporadically demonstrate mostly ill-defined or spiculated margins (28,30).

Our results are also in agreement with histopathologic data from the ovarian cancer literature (18,19). Reyes et al evaluated morphologic features of peritoneal implants in 102 HGSOC patients with known *BRCA* genotype. They found that 76% of *BRCA*-mutant HGSOC had peritoneal deposits with rounded or "pushing" contours, whereas all *BRCA* wild-type HGSOC had infiltrative peritoneal implants (18).

In general, little is known about the imaging manifestations of various genomic alterations in HGSOC. Vargas et al explored the relationships between CT features and CLOVAR (classification of ovarian cancer) subtypes of HGSOC (25). Similar to that study, we did not identify any significant associations between CT features of primary ovarian masses and gene mutation status (25). However, Vargas et al did find PD pattern and mesenteric infiltration to be associated with CLOVAR subtypes, and we also demonstrated PD pattern and mesenteric involvement to be associated with gene mutations, in our study with *BRCA* mutation status. Thus, it is possible that genomic alterations exert greater influence on the morphology of extraovarian implants than on primary ovarian masses. Future studies are needed to validate this hypothesis.

Second, we found none of the clinical characteristics or CT features to be associated with the results of primary cytoreductive surgery in *BRCA*-mutant HGSOC. In contrast, the presence

of PD in lesser sac and left upper quadrant, presence of mesenteric involvement, and lymphadenopathy in supradiaphragmatic and suprarenal para-aortic regions were associated with significantly higher odds of incomplete gross resection in *BRCA* wild-type HGSOC. It is possible that the infiltrative PD pattern we observed on CT scans of patients with *BRCA* wild-type HGSOC increases the difficulty of cytoreductive surgery by making it more challenging to visualize the tumor.

Several prior investigators have evaluated the value of preoperative CT in patients with epithelial ovarian cancer including HGSOC in an effort to identify imaging predictors of cytoreductive outcome (20,31–38). However, to our knowledge, none have evaluated CT indicators of cytoreductive outcome separately in patients with *BRCA*-mutant HGSOC and patients with *BRCA* wild-type HGSOC. Our data suggest that there may be an interaction between CT features, the result of primary surgical cytoreduction (complete vs incomplete cytoreduction), and *BRCA* mutation status, but our conclusions are limited by a relatively small sample size and require further validation.

Third, we found the presence of mesenteric involvement at CT to be associated with significantly shorter PFS for both patients with *BRCA*-mutant HGSOC (multiple regression) and patients with *BRCA* wild-type HGSOC (univariate analysis). Our results agree with the conclusions of Vargas et al who also identified a statistically significant association between the presence of mesenteric infiltration at CT and shorter PFS in patients with HGSOC (25). On the basis of these observations, further investigation of mesenteric involvement at preoperative CT as a prognostic biomarker may be warranted.

Our study had several limitations. First, it was a retrospective study and only some patients with HGSOC underwent *BRCA* testing from 2005 to 2008, potentially introducing a selection bias. Second, our study included a relatively small number of patients, particularly women with *BRCA*-mutant HGSOC. As a result, we could not evaluate separately patients with *BRCA1* and patients with *BRCA2* mutations. In some instances, risk estimates and multiple regression could not be conducted due to limited sample size. Third, because most patients underwent optimal debulking, we focused on the ability of clinical data and CT features to predict the odds of complete versus incomplete cytoreduction. Last, the time interval between preoperative CT and primary cytoreductive surgery was relatively long for one patient, which introduced a possibility of interval tumor growth. However, 107 of 108 (99%) patients underwent CT within 60 days of surgery.

In conclusion, *BRCA* mutation status was associated with potentially important differences in CT features; presence of mesenteric involvement at CT was a key indicator of shorter PFS in both groups.

Acknowledgment: Authors thank Joanne Chin, MFA, for her editorial assistance with the manuscript.

Disclosures of Conflicts of Interest: S.N. disclosed no relevant relationships. **Y.L.** disclosed no relevant relationships. **M.G.** disclosed no relevant relationships. **D.A.G.** disclosed no relevant relationships. **M.M.** disclosed no relevant relationships. **M.D.** disclosed no relevant relationships. **S.A.J.** disclosed no relevant relationships. **K.J.** disclosed no relevant relationships. **A.G.A.** disclosed no relevant relationships. **R.E.S.** disclosed no relevant relationships. **R.A.S.** disclosed no relevant relationships. **H.A.V.** disclosed no relevant relationships. **H.H.** disclosed no relevant relationships. **N.D.K.** disclosed no relevant relationships. **E.S.** disclosed no relevant relationships.

References

1. Siegel RL, Miller KD, Jemal A. Cancer statistics, 2017. CA Cancer J Clin 2017;67(1):7–30.
2. Hennessy BT, Coleman RL, Markman M. Ovarian cancer. Lancet 2009;374(9698):1371–1382.
3. Verhaak RG, Tamayo P, Yang JY, et al. Prognostically relevant gene signatures of high-grade serous ovarian carcinoma. J Clin Invest 2013;123(1):517–525.
4. Tothill RW, Tinker AV, George J, et al. Novel molecular subtypes of serous and endometrioid ovarian cancer linked to clinical outcome. Clin Cancer Res 2008;14(16):5198–5208.
5. Cancer Genome Atlas Research Network. Integrated genomic analyses of ovarian carcinoma. Nature 2011;474(7353):609–615. [Published correction appears in Nature 2012;490(7419):298.]
6. Hirsh-Yechezkel G, Chetrit A, Lubin F, et al. Population attributes affecting the prevalence of BRCA mutation carriers in epithelial ovarian cancer cases in israel. Gynecol Oncol 2003;89(3):494–498.
7. Risch HA, McLaughlin JR, Cole DE, et al. Prevalence and penetrance of germline BRCA1 and BRCA2 mutations in a population series of 649 women with ovarian cancer. Am J Hum Genet 2001;68(3):700–710.
8. Hyman DM, Zhou Q, Iasonos A, et al. Improved survival for BRCA2-associated serous ovarian cancer compared with both BRCA-negative and BRCA1-associated serous ovarian cancer. Cancer 2012;118(15):3703–3709.
9. Liu J, Cristea MC, Frankel P, et al. Clinical characteristics and outcomes of BRCA-associated ovarian cancer: genotype and survival. Cancer Genet 2012;205(1-2):34–41.
10. Artioli G, Borgato L, Cappetta A, et al. Overall survival in BRCA-associated ovarian cancer: case-control study of an Italian series. Eur J Gynaecol Oncol 2010;31(6):658–661.
11. Jóhannsson OT, Ranstam J, Borg A, Olsson H. Survival of BRCA1 breast and ovarian cancer patients: a population-based study from southern Sweden. J Clin Oncol 1998;16(2):397–404.
12. Chetrit A, Hirsh-Yechezkel G, Ben-David Y, Lubin F, Friedman E, Sadetzki S. Effect of BRCA1/2 mutations on long-term survival of patients with invasive ovarian cancer: the national Israeli study of ovarian cancer. J Clin Oncol 2008;26(1):20–25.
13. Boyd J, Sonoda Y, Federici MG, et al. Clinicopathologic features of BRCA-linked and sporadic ovarian cancer. JAMA 2000;283(17):2260–2265.
14. Yang D, Khan S, Sun Y, et al. Association of BRCA1 and BRCA2 mutations with survival, chemotherapy sensitivity, and gene mutator phenotype in patients with ovarian cancer. JAMA 2011;306(14):1557–1565.
15. Gallagher DJ, Konner JA, Bell-McGuinn KM, et al. Survival in epithelial ovarian cancer: a multivariate analysis incorporating BRCA mutation status and platinum sensitivity. Ann Oncol 2011;22(5):1127–1132.
16. Scheuer L, Kauff N, Robson M, et al. Outcome of preventive surgery and screening for breast and ovarian cancer in BRCA mutation carriers. J Clin Oncol 2002;20(5):1260–1268.

17. Grann V, Ashby-Thompson M. Role of genetic testing for screening and prevention for ovarian cancer: comment on "Risk-reducing salpingo-oophorectomy and ovarian cancer screening in 1077 women after BRCA testing". JAMA Intern Med 2013;173(2):103–104.

18. Reyes MC, Arnold AG, Kauff ND, Levine DA, Soslow RA. Invasion patterns of metastatic high-grade serous carcinoma of ovary or fallopian tube associated with BRCA deficiency. Mod Pathol 2014;27(10):1405–1411.

19. Soslow RA, Han G, Park KJ, et al. Morphologic patterns associated with BRCA1 and BRCA2 genotype in ovarian carcinoma. Mod Pathol 2012;25(4):625–636.

20. Suidan RS, Ramirez PT, Sarasohn DM, et al. A multicenter prospective trial evaluating the ability of preoperative computed tomography scan and serum CA-125 to predict suboptimal cytoreduction at primary debulking surgery for advanced ovarian, fallopian tube, and peritoneal cancer. Gynecol Oncol 2014;134(3):455–461.

21. Vargas HA, Burger IA, Goldman DA, et al. Volume-based quantitative FDG PET/CT metrics and their association with optimal debulking and progression-free survival in patients with recurrent ovarian cancer undergoing secondary cytoreductive surgery. Eur Radiol 2015;25(11):3348–3353.

22. Zivanovic O, Sima CS, Iasonos A, et al. The effect of primary cytoreduction on outcomes of patients with FIGO stage IIIC ovarian cancer stratified by the initial tumor burden in the upper abdomen cephalad to the greater omentum. Gynecol Oncol 2010;116(3):351–357.

23. Naik R, Spirtos N, Pomel C, et al. The "definitive" trial of surgical cytoreduction in advanced-stage ovarian cancer. Int J Gynecol Cancer 2013;23(4):588–591.

24. Gilks CB, Ionescu DN, Kalloger SE, et al. Tumor cell type can be reproducibly diagnosed and is of independent prognostic significance in patients with maximally debulked ovarian carcinoma. Hum Pathol 2008;39(8):1239–1251.

25. Vargas HA, Miccò M, Hong SI, et al. Association between morphologic CT imaging traits and prognostically relevant gene signatures in women with high-grade serous ovarian cancer: a hypothesis-generating study. Radiology 2015;274(3):742–751.

26. Eisenhauer EA, Therasse P, Bogaerts J, et al. New response evaluation criteria in solid tumours: revised RECIST guideline (version 1.1). Eur J Cancer 2009;45(2):228–247.

27. Rustin GJ, Marples M, Nelstrop AE, Mahmoudi M, Meyer T. Use of CA-125 to define progression of ovarian cancer in patients with persistently elevated levels. J Clin Oncol 2001;19(20):4054–4057.

28. Veltman J, Mann R, Kok T, et al. Breast tumor characteristics of BRCA1 and BRCA2 gene mutation carriers on MRI. Eur Radiol 2008;18(5):931–938.

29. Kaas R, Kroger R, Peterse JL, Hart AA, Muller SH. The correlation of mammographic-and histologic patterns of breast cancers in BRCA1 gene mutation carriers, compared to age-matched sporadic controls. Eur Radiol 2006;16(12):2842–2848.

30. Kaas R, Kroger R, Hendriks JH, et al. The significance of circumscribed malignant mammographic masses in the surveillance of BRCA 1/2 gene mutation carriers. Eur Radiol 2004;14(9):1647–1653.

31. Qayyum A, Coakley FV, Westphalen AC, Hricak H, Okuno WT, Powell B. Role of CT and MR imaging in predicting optimal cytoreduction of newly diagnosed primary epithelial ovarian cancer. Gynecol Oncol 2005;96(2):301–306.

32. Jung DC, Kang S, Kim MJ, Park SY, Kim HB. Multidetector CT predictors of incomplete resection in primary cytoreduction of patients with advanced ovarian cancer. Eur Radiol 2010;20(1):100–107.

33. Ferrandina G, Sallustio G, Fagotti A, et al. Role of CT scan-based and clinical evaluation in the preoperative prediction of optimal cytoreduction in advanced ovarian cancer: a prospective trial. Br J Cancer 2009;101(7):1066–1073.

34. Nelson BE, Rosenfield AT, Schwartz PE. Preoperative abdominopelvic computed tomographic prediction of optimal cytoreduction in epithelial ovarian carcinoma. J Clin Oncol 1993;11(1):166–172.

35. Meyer JI, Kennedy AW, Friedman R, Ayoub A, Zepp RC. Ovarian carcinoma: value of CT in predicting success of debulking surgery. AJR Am J Roentgenol 1995;165(4):875–878.

36. Bristow RE, Duska LR, Lambrou NC, et al. A model for predicting surgical outcome in patients with advanced ovarian carcinoma using computed tomography. Cancer 2000;89(7):1532–1540.

37. Axtell AE, Lee MH, Bristow RE, et al. Multi-institutional reciprocal validation study of computed tomography predictors of suboptimal primary cytoreduction in patients with advanced ovarian cancer. J Clin Oncol 2007;25(4):384–389.

38. Dowdy SC, Mullany SA, Brandt KR, Huppert BJ, Cliby WA. The utility of computed tomography scans in predicting suboptimal cytoreductive surgery in women with advanced ovarian carcinoma. Cancer 2004;101(2):346–352.